

A HIGH-RESOLUTION VIEW OF THE ORIENTALE BASIN AND SURROUNDINGS FROM THE GRAVITY RECOVERY AND INTERIOR LABORATORY (GRAIL). Maria T. Zuber¹, David E. Smith¹, Sander J. Goossens², Sami W. Asmar³, Alexander S. Konopliv³, Frank G. Lemoine⁴, H. Jay Melosh⁵, Gregory A. Neumann⁴, Roger J. Phillips⁶, Sean C. Solomon^{7,8}, Michael M. Watkins³, Mark A. Wieczorek⁹, Jeffrey C. Andrews-Hanna¹⁰, James W. Head¹¹, Walter S. Kiefer¹², Patrick J. McGovern¹², Francis Nimmo¹³, G. Jeffrey Taylor¹⁴, Jonathan Besserer¹³, Brandon C. Johnson⁵, Katarina Miljković⁹, Jason M. Soderblom¹, David M. Blair⁵, Gerhard L. Krüzinga³, Erwan Mazarico^{1,4}, Dah-Ning Yuan³. ¹Department of Earth, Atmospheric and Planetary Sciences, Massachusetts Institute of Technology, Cambridge, MA 02129, USA (zuber@mit.edu); ²University of Maryland, Baltimore County, Baltimore, MD 21250, USA. ³Jet Propulsion Laboratory, California Institute of Technology, Pasadena, CA 91109-8099, USA; ⁴NASA Goddard Space Flight Center, Greenbelt, MD 20771, USA; ⁵Department of Earth, Atmospheric, and Planetary Sciences, Purdue University, West Lafayette, IN 47907, USA; ⁶Planetary Science Directorate, Southwest Research Institute, Boulder, CO 80302, USA; ⁷Lamont-Doherty Earth Observatory, Columbia University, Palisades, NY 10964, USA; ⁸Department of Terrestrial Magnetism, Carnegie Institution of Washington, Washington, DC 20015, USA; ⁹Institut de Physique du Globe de Paris, 94100 Saint Maurice des Fossés, France; ¹⁰Department of Geophysics and Center for Space Resources, Colorado School of Mines, Golden, CO 80401, USA; ¹¹Department of Geological Sciences, Brown University, Providence, RI 02912, USA; ¹²Lunar and Planetary Institute, Houston, TX 77058, USA; ¹³Department of Earth and Planetary Sciences, University of California, Santa Cruz, CA 95064, USA; ¹⁴Hawaii Institute of Geophysics and Planetology, University of Hawaii, Honolulu, HI 96822, USA;

Introduction: During the final weeks (the “end-game”) of the Gravity Recovery and Interior Laboratory (GRAIL) mission [1], the orbital altitude of the dual spacecraft was lowered to an average of 11 km above the surface of the Moon. The endgame mapping strategy [2] was designed to provide the highest-resolution coverage over the Orientale basin in order to provide a gravity map of a multi-ring impact basin at unprecedented resolution. (High-resolution data over other areas of the planet were acquired as well.) Here we summarize methodology and present results of local analysis to produce a gravitational model with 3-5-km spatial resolution, appropriate for investigating the structure and evolution of Orientale and its surroundings.

GRAIL Modeling Status: GRAIL [1], a twin-spacecraft lunar gravity mission, was launched on September 10, 2012, and mapped the Moon at decreasing altitudes in sequential orbital phases, until its planned de-orbit on December 17, 2012. Initial analysis of data acquired during the Primary Mission (PM) [3] at a mean orbital altitude of 55 km led to a global spherical harmonic model (GL0420A) of the gravitational field to degree and order 420 (spatial block size = 13 km) [4] that represented an improvement in spatial resolution by a factor of 3-4 and in quality by three to more than five orders of magnitude over previous models from all earlier missions. Subsequent PM spherical harmonic models achieved degree and order 660 (spatial block size = 8.2 km) [5, 6]. During GRAIL’s Extended Mission (XM), the mapping altitude was lowered by a factor of two to 23 km; the highest resolution global gravity field so far achieved is to degree and

order 1080 (spatial block size = 5 km) [7], but in practice that resolution is achieved only at the lowest mapping altitudes. On December 6, 2012, the average altitude of the two GRAIL orbiters was lowered by another factor of two, to 11 km. This maneuver enabled a very high-resolution mapping campaign over the Orientale basin (among other regions) during which time the twin spacecraft orbited to within 2 km of the surface of the basin’s rings.

Local Solution for Orientale: In order to achieve the highest-resolution gravitational model of Orientale, we performed [8] a short-arc analysis [9] of GRAIL’s Ka-band range rate (KBRR) observations by adjusting *a priori* field GRGM900A while embedding neighbor smoothing [10, 11]. KBRR residuals with respect to GRGM900A before and after the local modeling are shown in Fig. 1 and illustrate the improvement in the local model. Free-air anomalies (Fig. 2) were constructed from mixed 1/6° and 1/10° grids. Our local analysis removes high-frequency striping as well as extends the resolution of anomalies in Orientale and its environs to 3-5 km, suitable for detailed investigations of basin origin and evolution.

Comparison with Previous Models: In previous analyses of the structure and compensation of Orientale [e.g., 12-15], the resolution of gravity was a limiting factor. In addition, it is now known that pre-GRAIL models under-sampled the Moon’s gravitational power even at wavelengths that were then thought to be well resolved [cf. 4]. Combination of GRAIL gravity with a 1/256° geodetically referenced topography [16] from the Lunar Orbiter Laser Altimeter (LOLA) [17] is permitting study of interior struc-

ture at the level of basin substructures. Analyses in progress include the mare, crustal and underlying upper mantle structure [e.g., 18-20], as well as the nature of rings as relevant to basin formation [cf. 21] and assessing predicted distributions of impact melt [22].

References: [1] Zuber M. T. et al. (2013) *Space Sci. Rev.* 178, 3-24, doi:10.1007/s11214-012-9952-7. [2] Sweetser T. H. et al. (2012) *AIAA Astrodyn. Specialist Conf.*, paper AIAA-2012-4429, Minneapolis, MN. [3] Roncoli R. B. and Fuji K.K. (2010) *AIAA Guidance, Navigation & Control Conf.*, paper AIAA 2010-9393, Toronto, Ontario, Canada. [4] Zuber M. T. et al. (2013) *Science* 339, 668-671, doi:10.1126/science.1231507. [5] Konopliv A. S. et al. (2013) *J. Geophys. Res. Planets* 118, 1415-1434, doi:10.1002/jgre.20097. [6] Lemoine F. G. et al. (2013) *J. Geophys. Res. Planets* 118, 1676-1698, doi:10.1002/jgre.20118. [7] Konopliv A. S. et al. (2013) *Geophys. Res. Lett.*, submitted. [8] Goossens S. et al. (2013) *Eos Trans. Am. Geophys. Un.*, Fall Meeting, G31-B. [9] Rowlands D. D. et al. (2002) *J. Geod.* 76, 307-316. [10] Rowlands D. D. et al. (2010) *J. Geophys. Res.* 115, B01403, doi:10.1029/2009JB006546.

[11] Sabaka T. J. et al. (2010) *J. Geophys. Res.* 115, B11403, doi:10.1029/2010JB007533. [12] Bratt S. R. et al. (1985) *J. Geophys. Res.* 90, 3049-3064, doi:10.1029/JB090iB04p03049. [13] Neumann G. A. et al. (1996) *J. Geophys. Res.* 101, 16,841-16,863. [14] von Frese R. B. et al. (1996) *J. Geophys. Res.* 102, 25,657-25,676. [15] Andrews-Hanna J. C. (2013) *Icarus* 222, 159-168, doi:10.1016/j.icarus.2012.10.031. [16] Smith D. E. et al. (2010) *Geophys. Res. Lett.* 37, L18204, doi:10.1029/2010GL043751. [17] Smith D. E. et al. (2010) *Space Sci. Rev.* 150, 209-241, doi:10.1007/s11214-009-9512-y. [18] Wieczorek M. A. et al. (2013) *Science* 339, 671-675, doi:10.1126/science.1231530. [19] Melosh H. J. et al. (2013) *Science* 340, 1552-1555, doi:10.1126/science.1235768. [20] Besserer J. et al. (2014) *Science*, submitted. [21] Melosh H. J. (1989) *Impact Cratering*, Oxford Univ. Press, 245 pp. [22] Vaughan W. M. (2013) *Icarus* 223, doi:10.1016/j.icarus.2013.01.017.

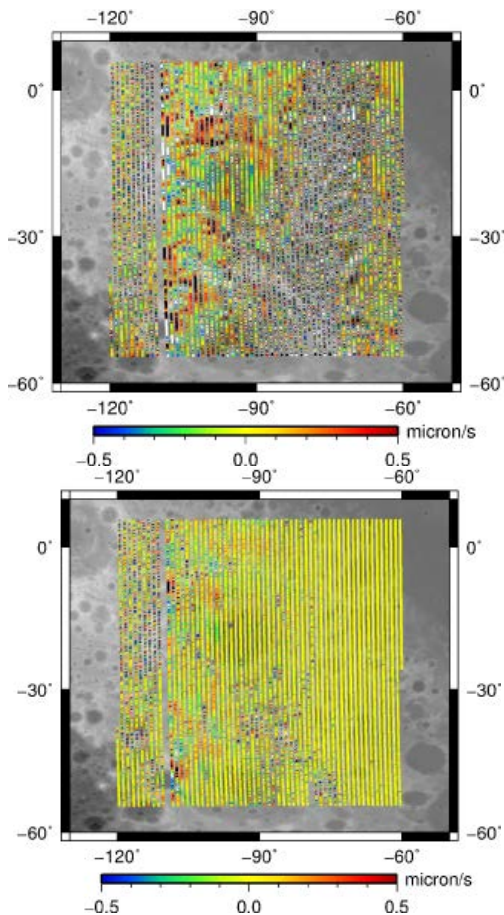


Figure 1. KBRR post-fit residuals along orbit tracks to (top) GRAIL gravity field GRGM900A and (bottom) local solution 1800 [8].

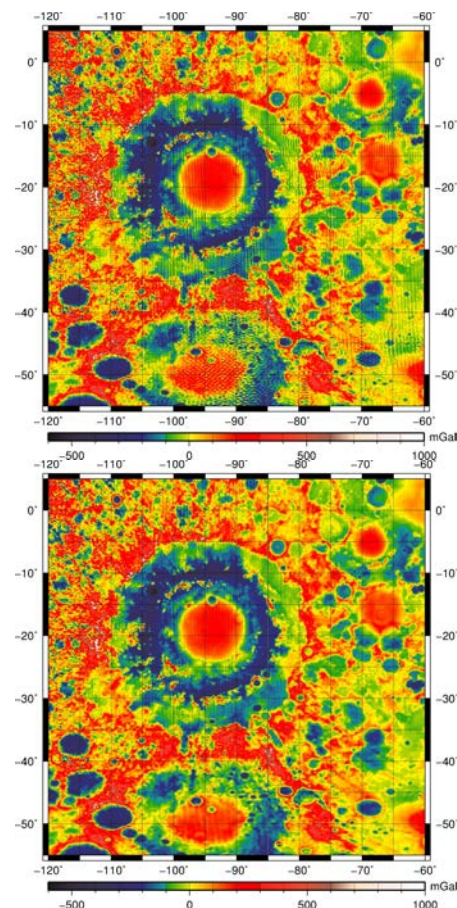


Figure 2. Free-air gravity of Orientale basin and surroundings from (top) GRAIL field GRGM900A and (bottom) local solution 1800 [8].